



Article

Bis-Phenoxo-Cu^{II}₂ Complexes: Formal Aromatic Hydroxylation via Aryl-Cu^{III} Intermediate Species

Xavi Ribas ^{1,*}, Raül Xifra ¹ and Xavier Fontrodona ²

¹ Institut de Química Computacional i Catàlisi and Departament de Química, Universitat de Girona, Campus Montilivi, E-17003 Girona, Catalonia, Spain; rxifra@cidqo.com

² Serveis Tècnics de Recerca (STR), Universitat de Girona, Parc Científic i Tecnològic, E-17003 Girona, Catalonia, Spain; xavier.fontrodona@udg.edu

* Correspondence: xavi.ribas@udg.edu; Tel.: +34-683-376-923

Academic Editors: Andreas A. Danopoulos and Georgios C. Vougioukalakis

Received: 8 September 2020; Accepted: 5 October 2020; Published: 9 October 2020



Abstract: Ullmann-type copper-mediated aryl-C-O bond formation has attracted the attention of the catalysis and organometallic communities, although the mechanism of these copper-catalyzed coupling reactions remains a subject of debate. We have designed well-defined triazamacrocyclic-based aryl-Cu^{III} complexes as an ideal platform to study the C-heteroatom reductive elimination step with all kinds of nucleophiles, and in this work we focus our efforts on the straightforward synthesis of phenols by using H₂O as nucleophile. Seven well-defined aryl-Cu^{III} complexes featuring different ring size and different electronic properties have been reacted with water in basic conditions to produce final bis-phenoxo-Cu^{II}₂ complexes, all of which are characterized by XRD. Mechanistic investigations indicate that the reaction takes place by an initial deprotonation of the NH group coordinated to Cu^{III} center, subsequent reductive elimination with H₂O as nucleophile to form phenoxo products, and finally air oxidation of the Cu^I produced to form the final bis-phenoxo-Cu^{II}₂ complexes, whose enhanced stability acts as a thermodynamic sink and pushes the reaction forward. Furthermore, the corresponding triazamacrocyclic-Cu^I complexes react with O₂ to undergo 1e⁻ oxidation to Cu^{II} and subsequent C-H activation to form aryl-Cu^{III} species, which follow the same fate towards bis-phenoxo-Cu^{II}₂ complexes. This work further highlights the ability of the triazamacrocyclic-Cu^{III} platform to undergo aryl-OH formation by reductive elimination with basic water, and also shows the facile formation of rare bis-phenoxo-Cu^{II}₂ complexes.

Keywords: organometallic Cu^{III}; C-O cross coupling; phenol synthesis; phenoxo-bridged Cu^{II} complexes; aromatic hydroxylation; copper

1. Introduction

Fundamental mechanistic understanding of Ullmann-type aryl-heteroatom cross-coupling chemistry is still scarce and difficult to obtain in actual catalytic systems, due to the elusive formation of very reactive intermediate species [1–7]. Methodological approaches consist of extensive optimization protocols to finally reach an effective method to obtain the desired reaction and performance [8–10], at the expense of intrinsic mechanistic understanding. Indeed, spectroscopic monitoring of the reactions is precluded by the use of high concentrated solutions and heterogeneous bases. It is proposed that complex mixtures of copper-complexes are involved, and that several mechanisms can be active in parallel. Nevertheless, one of the most accepted mechanisms involves a 2e⁻-Cu^I/Cu^{III} catalytic cycle via the classical oxidative addition/reductive elimination steps [7,11].

A successful strategy to overcome the problem of mechanistic understanding is the design of macrocyclic substrate scaffolds to tame the reactivity of the intermediate copper species [7,10,12]. In this manner, well-defined aryl-Cu^{III} key intermediate species have been isolated and crystallized,

and their reactivity in reductive elimination processes with heteroatom nucleophiles (O, N, S, Se, P) has been widely studied [11–23]. In addition, upgrading to catalytic C-Heteroatom cross couplings has been proved in some of them [7,11,21]. A particularly interesting type of nucleophiles are those bearing O-heteroatoms, which streamline the synthesis of biaryl ethers and aryl-alkyl ethers [24–26], and this copper-catalyzed reactivity has proved to be very effective [8,27]. In this regard, we reported a detailed mechanistic investigation on the reactivity of well-defined triazamacrocyclic aryl-Cu^{III} species with HO-nucleophiles (HONuc = carboxylic acids, phenols and aliphatic alcohols) [26]. These reactions afforded the corresponding aryl-O-Nuc products under mild conditions, via a reductive elimination path.

A remarkable case of C-O coupling is the synthesis of phenol (aryl-OH), since this would imply the use of water as a nucleophile. Actually, the current synthetic methods of phenol include the classical non-metal-catalyzed transformations, such as (a) the oxidation of aryl aldehydes or aryl ketones with H₂O₂ (Dakin reaction) [28] and (b) the reaction of water with diazo-aryl compounds (Sandmeyer reaction) [29], and the transition metal-catalyzed transformations, such as (c) Pd-catalyzed cross coupling reactions using H₂O [30,31] and (d) Cu-catalyzed cross coupling reactions using H₂O [32,33], among many others [34–36].

In this work, we study the reactivity of well-defined triazamacrocyclic aryl-Cu^{III} species with water to evaluate the possibility to synthesize phenol products and to understand the mechanistic details of this coupling. The triazamacrocyclic aryl-Cu^{III} species can be obtained via two synthetic strategies: (1) quantitative formation via Cu^I oxidative addition with triazamacrocyclic aryl-X substrates (Figure 1a) [11,16,23], or (2) via C-H activation and metalation with Cu^{II} using triazamacrocyclic aryl-H substrates and further disproportionation to afford equimolar amounts of the desired aryl-Cu^{III}, Cu^I salt and protonated substrate (Figure 1b) [16,37]. The unreported reactivity of the well-defined aryl-Cu^{III} complexes with water in basic conditions is presented in this work, leading to aryl-OH coupling species, a formal aromatic hydroxylation of arenes. The crystal structures of the final bis-phenoxo-Cu^{II}₂ complexes nicely show the effectivity of the C-O reductive elimination at Cu^{III} and the easy oxidation of the resulting Cu^I to bis-phenoxo-Cu^{II}₂ complexes as thermodynamic sink.

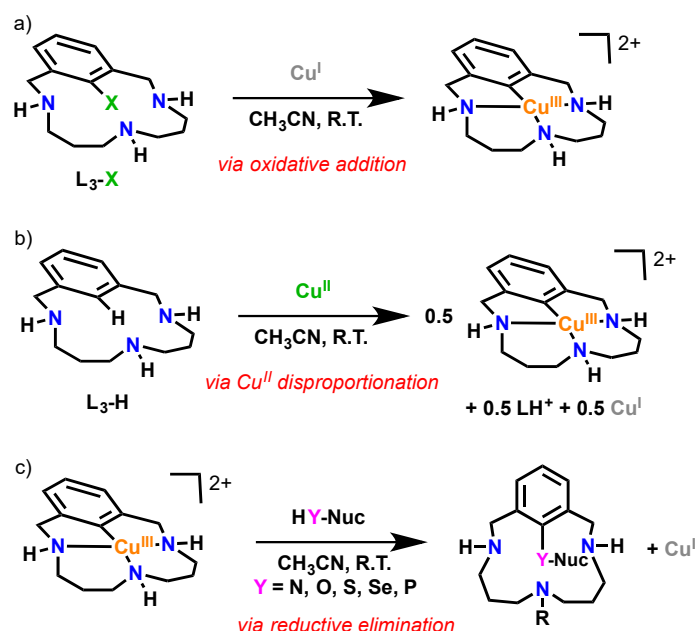


Figure 1. Fundamental organometallic reaction features by triazamacrocyclic ligands (L₃-X and L₃-H shown). (a) Quantitative formation of aryl-Cu^{III} complex through oxidative addition at Cu^I with L₃-X (X = Cl, Br, I). (b) Equimolar formation of aryl-Cu^{III} complex and Cu^I through Cu^{II} disproportionation upon aromatic C-H activation of L₃-H at Cu^{II}. (c) C-Heteroatom bond formation through reductive elimination of HY-Nuc (Y = N, O, S, Se, P) with the aryl-Cu^{III} complex.

2. Results and Discussion

2.1. Aryl-Cu^{III} Complexes and Their Reactivity with Basic Water

The well-defined macrocyclic aryl-Cu^{III} complexes (**1**_{L1}–**1**_{L3}) used in this work were prepared following our reported protocols [11,16,23,24,37].

Complexes [(L_x)Cu^{III}](X)₂ (x = 1–3; X = ClO₄[−], OTf[−], PF₆[−]) dissolved in CH₃CN react with one equivalent of aqueous KOH 1M at room temperature to give colored intermediates (Figure 2, route a). Solution acquires a red-brown (when L₁ is used) or deep-violet (when L₂–L₃ is used) color, which fade to obtain final green solutions. Colored intermediates take 2–3 h to totally fade to green products. Slow diethyl ether diffusion leads to the final bis-phenoxo complexes as green crystals: [(L₁-O)₂Cu^{II}]₂(OTf)₂ (**3**_{L1}-(OTf)₂) in 30% isolated yield, [(L₂-O)₂Cu^{II}]₂(X)₂ (**3**_{L2}-(X)₂, X = OTf, ClO₄) in 65% yield and [(L₃-O)₂Cu^{II}]₂(PF₆)₂ (**3**_{L3}-(PF₆)₂) in 60% yield.

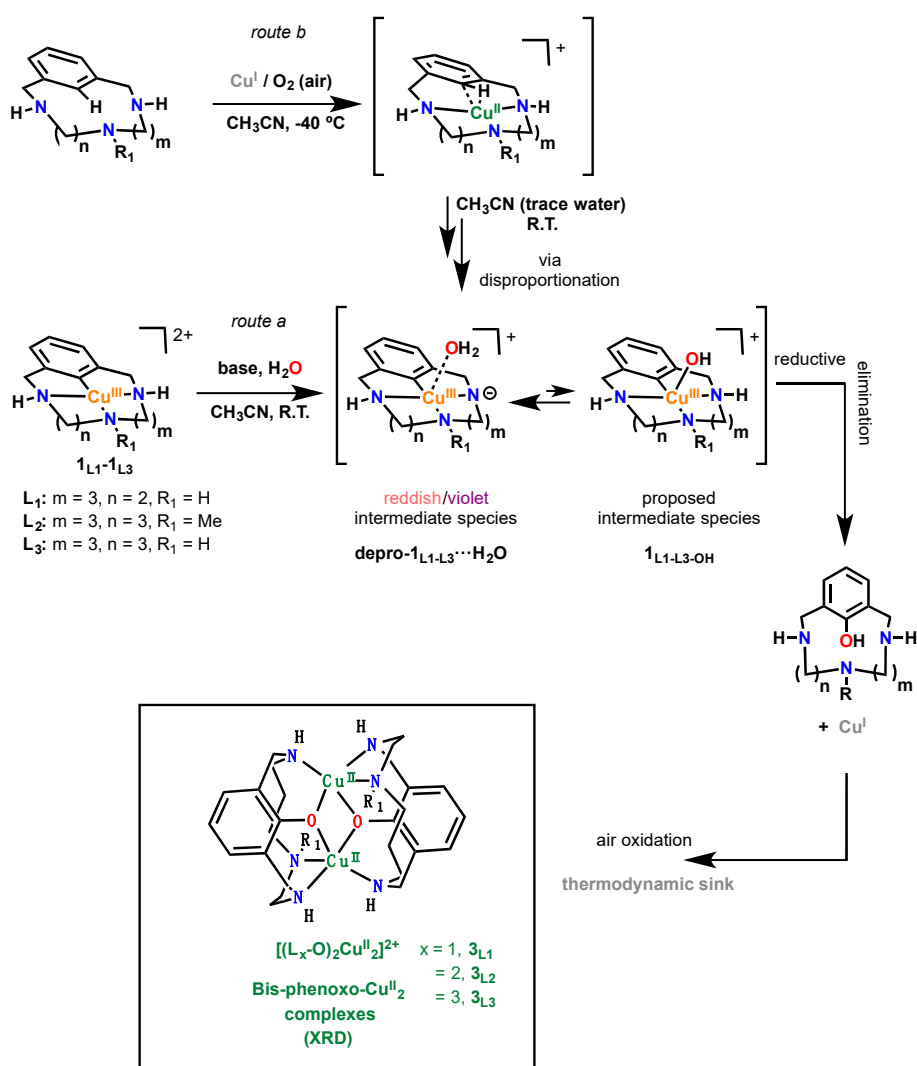


Figure 2. Reactivity of aryl-Cu^{III} complexes with basic water (**route a**) through initial deprotonation, axial coordination of H₂O, internal deprotonation of water to hydroxide and reductive elimination to form the aryl-OH products and Cu^I. Subsequent air oxidation of Cu^I to Cu^{II} causes the formation of the very stable bis-phenoxo-Cu^{II}₂ final complexes. On the upper part of the figure (**route b**), the same colored deprotonated aryl-Cu^{III} species can be obtained through Cu^I/air reaction via concomitant C-H activation and disproportionation at Cu^{II}. These reactions are featured with triazamacrocyclic systems L₁–L₃.

The structures are all analogous and consist of a dimetallic Cu^{II} complex showing a N_3O_2 distorted trigonal bipyramidal geometry for each metal, where the two phenoxo groups are bridging and the three amine moieties belong to the two ligands featured in the structure.

2.2. X-ray Diffraction Analysis of the Bis-Phenoxo- Cu^{II} ₂ Complexes (**3**_{L1}–**3**_{L3})

Crystal structure for complex $[(\text{L}_1\text{-O})_2\text{Cu}^{\text{II}}_2](\text{OTf})_2$ (**3**_{L1}-(OTf)₂) was obtained, and its ORTEP diagram is shown in Figure 3a. The molecule sits on a symmetrical center that transforms one macrocyclic ligand into the other. Each copper metal atom has a strongly distorted trigonal bipyramidal towards a square-planar pyramidal geometry (with a τ factor [38] of 0.56), and can be considered a mixture of both. Copper centers share coordinative sites with both ligands. Each copper atom is coordinated to a phenoxo O atom and an N atom from one of the macrocyclic ligands, and to the phenoxo O atom and two N atoms from the second macrocyclic ligand. The copper metal centers become doubly bridged by each macrocyclic ligand. The oxygen atoms of the phenoxo groups are bridging the copper metal centers so that the axial oxygen atom from one pyramid also occupies a position in the trigonal base of the other pyramid. The Cu_2O_2 core atoms lie in a plane forming a rhomboidal arrangement (Cu–O 1.930(2) Å, 2.174(2) Å), Cu⋯Cu 3.085 Å and O⋯O 2.718 Å).

Structures of complexes $[(\text{L}_2\text{-O})_2\text{Cu}^{\text{II}}_2](\text{ClO}_4)_2\cdot\text{CH}_3\text{CN}$ (**3**_{L2}-(ClO₄)₂·CH₃CN) and $[(\text{L}_3\text{-O})_2\text{Cu}^{\text{II}}_2](\text{PF}_6)_2$ (**3**_{L3}-(PF₆)₂) were also determined by X-ray diffraction (Figure 3b,c, respectively). Both dinuclear structures **3**_{L2} and **3**_{L3} bear the same ligand-donor set N_3O_2 per Cu atom and copper metal centers become doubly bridged by each macrocyclic ligand, as the previously described complex **3**_{L1}. Each copper metal atom in complexes **3**_{L2} and **3**_{L3} has a strongly distorted trigonal bipyramidal towards a square-planar pyramidal geometry (with a τ factor of 0.61 for **3**_{L2} and 0.62 for **3**_{L3}), featuring the same macrocyclic ligand size (14-membered). The oxygen atoms of the phenoxo groups in complex **3**_{L2} are bridging the copper metal centers so that the axial oxygen atom from one pyramid also occupies a position in the trigonal base of the other pyramid. The Cu_2O_2 core atoms lie in a plane forming a rhomboidal arrangement (Cu–O 1.925(1) Å, 2.128(2) Å, Cu⋯Cu 3.132 Å and O⋯O 2.581 Å). A rhomboidal arrangement of the Cu_2O_2 core is also found for complex **3**_{L3} (Cu–O 1.930(3) Å, 2.122(3) Å, Cu⋯Cu 3.103 Å and O⋯O 2.613 Å).

These structures are very rare, and to our knowledge there is only one precedent in the literature, reported in 2002 [39], where a small (12-membered) triazamacrocycle ($\text{L}_4\text{-H}$, $m = 2$, $n = 2$, $\text{R}_1 = \text{H}$) already showed the ability to form a bis-phenoxo- Cu^{II} ₂ compound through route b (Figure 2), but no aryl- Cu^{III} was detected, probably due to its small size and its inability to accommodate aryl- Cu^{III} intermediate species. Contrary to the structures reported in this work, the smaller macrocycle favored a more square-planar geometry for each copper center (with a τ factor of 0.21).

The comparison of crystal structures of these complexes shows the same type of N_3O_2 coordination sphere for each Cu atom, although geometry environment for copper is directly related to conformational constraints imposed by ligand backbone. Thus, the trend found shows that the smaller size of the macrocycle favors square-pyramidal geometry (12-membered L_4 , τ factor of 0.21) [39], whereas 13-membered L_1 afforded a τ factor of 0.56, and 14-membered macrocyclic rings (L_2 – L_3) showed τ values in the range of 0.60–0.67.

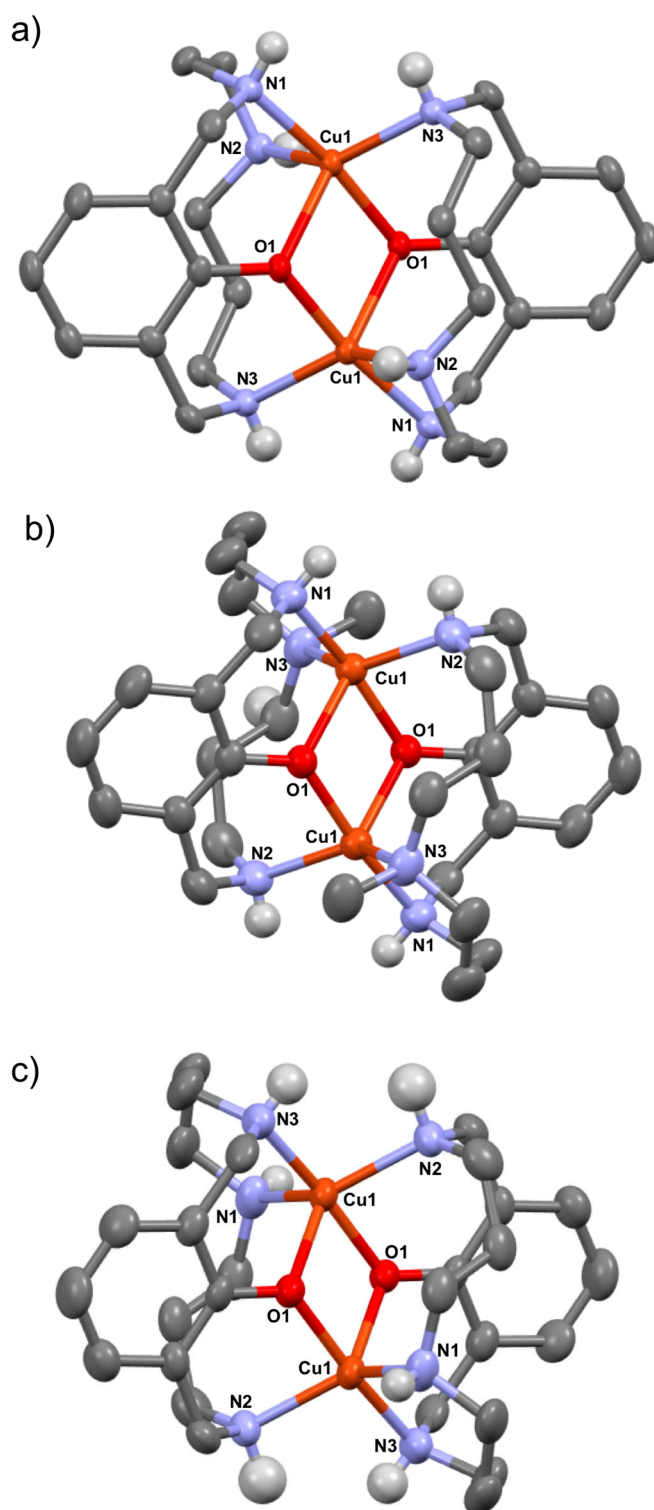


Figure 3. ORTEP diagrams corresponding to the cationic fragments of complexes (a) $[(L_1-O)_2Cu^{II}_2](OTf)_2$ ($3_{L1}-(OTf)_2$), (b) $[(L_2-O)_2Cu^{II}_2](ClO_4)_2 \cdot CH_3CN$ ($3_{L2}-(ClO_4)_2 \cdot CH_3CN$) and (c) $[(L_3-O)_2Cu^{II}_2](PF_6)_2$ ($3_{L3}-(PF_6)_2$) (only hydrogen atoms from NH moieties are shown and atoms coordinating to Cu are labelled for clarity).

2.3. Mechanistic Investigation on the Aromatic Hydroxylation Reaction

In order to gain more mechanistic insight of the C-O coupling by reaction of aryl-Cu^{III} with water under basic conditions, the synthetic conditions have been optimized for the synthesis [(L₂-O)₂Cu^{II}]₂(ClO₄)₂ (**3**_{L2}-(ClO₄)₂). In principle, any aqueous base reagent instead of KOH 1 M can be used to achieve the final product, as shown in Table 1. Interestingly, other O-containing reagents such as H₂O₂ are also able to perform the hydroxylation reaction. However, the addition of H₂O₂ 3% in water did not cause any change to copper(III) until the base Et₃N was injected into the solution (see entries 6–7 in Table 1). From these series of reactions, it may be concluded that the addition of water or H₂O₂ does not affect the stability of the aryl-Cu^{III}, and only the presence of a base triggers the reaction to bis-phenoxo complex formation through a colored intermediate. The presence of O₂ in the solution in entry 5 was tested to check if it had any influence in reaction time-scale or final yield. No quenching of violet intermediate was found but differences in final yield were noticeable: 20% yield for reaction (entry 5) and 53% for entry 3. When using the hydrogen peroxide activated with DABCO (entries 8–9), we noticed that product **3**_{L2} was obtained in substantially better yield (40%, entry 9) when 0.5 equivalents of the DABCO.2H₂O₂ adduct were used.

Table 1. Different reactivity behavior of [(L₂)Cu^{III}](OTf)₂ (**1**_{L2}) in front of different bases and water content to finally obtain **3**_{L2}. Typical experiment conditions: CH₃CN, [Cu^{III}] = 5–20 mM, N₂ atmosphere (unless change specified), R.T. Traces of water are always present.

Entry	Reagents	Reaction Time (min)	Isolated Yield of 3 _{L2} (%)
1	KOH (1 eq.), H ₂ O (54 eq.)	60 min	65%
2	KOH (2 eq.), H ₂ O (108 eq.)	25 min	8%
3	Proton Sponge (1 eq.), H ₂ O (7 eq.)	180 min	53%
4	Proton Sponge (1 eq.)	60 min	0%
5	Proton Sponge (1 eq.), O ₂ (excess)	240 min	20%
6	H ₂ O ₂ (3% in H ₂ O) (1 eq.), H ₂ O (52 eq.), Et ₃ N (1 eq.)	10 min	31%
7	H ₂ O ₂ (3% in H ₂ O) (1 eq.), H ₂ O (52 eq.)	60 min	0%
8	DABCO.2H ₂ O ₂ (2 eq.)	45 min	15%
9	DABCO.2H ₂ O ₂ (0.5 eq.)	40 min	40%

The colored intermediate was characterized by UV-vis and corresponded to the deprotonated aryl-Cu^{III} species for L₁–L₃ systems (Figure 4), analogously to the reported case of deprotonated-**1**_{L2} complex (depro-**1**_{L2}) [40]. In addition, weak axial coordination of a water molecule to the Cu^{III} center is proposed as a necessary species towards C-O reductive elimination. The same reactivity behavior is found for complex [(L₃)Cu^{III}]²⁺, whereas significant differences are shown by complex [(L₁)Cu^{III}]²⁺. For the latter, stability of red-brown intermediate depro-**1**_{L1} is much higher than for depro-**1**_{L2}, depro-**1**_{L3}, and reaction is not finished in less than 24 h upon KOH addition. In line with the enhanced stability, a significantly lower yield (30%) for the corresponding bis-phenoxo complex [(L₁-O)₂Cu^{II}]₂²⁺ (**3**_{L1}) was found.

2.4. Aromatic Hydroxylation via Arene C-H Activation with Cu^I/O₂

The study of dioxygen activation by the Cu^I complexes synthesized with ligands L₁–L₃ demonstrated another mechanistic twist regarding formal aromatic C-H hydroxylations. Bubbling O₂ to [(L₁-H)Cu^I](OTf) (**2**_{L1-H}), [(L₂-H)Cu^I](OTf) (**2**_{L2-H}), and [(L₃-H)Cu^I](OTf) (**2**_{L3-H}) at room temperature in CH₃CN caused the formation of intense colored intermediates resembling intermediates depro-**1**_{L1}, depro-**1**_{L2}, and depro-**1**_{L3}, respectively (Figure 2, route b). Besides, decomposition of colored intermediates gives the same bis-phenoxo copper(II) complexes [(L₁-O)₂Cu^{II}]₂²⁺ (**3**_{L1}), [(L₂-O)₂Cu^{II}]₂²⁺ (**3**_{L2}) and [(L₃-O)₂Cu^{II}]₂²⁺ (**3**_{L3}) as final products, although in significantly lower yields (25% isolated yield for **3**_{L2}). The UV-vis monitoring of these reactions confirmed that hydroxylation was occurring through the same aryl-Cu^{III} intermediates, featuring the same LMCT bands in each case, albeit with lower intensities. In addition, ¹H NMR monitoring of the O₂ bubbling to [(L₁-H)Cu^I](OTf) (**2**_{L1-H}) in

CD₃CN clearly shows the formation of peaks corresponding to depro-1_{L1} after 30 min (see Figure S1 in the Supplementary Materials), reaching full formation above 10 h [11,40]. The ESI-MS spectrum for violet intermediate obtained by reacting [(L₃-H)Cu^I]⁺ with O₂ shows a characteristic peak at *m/z* = 294 corresponding to the fragment depro-1_{L3} (see Figure S2). Under these conditions, decomposition of the intermediate towards 3_{L2} formation was slow and was detected after 40 h.

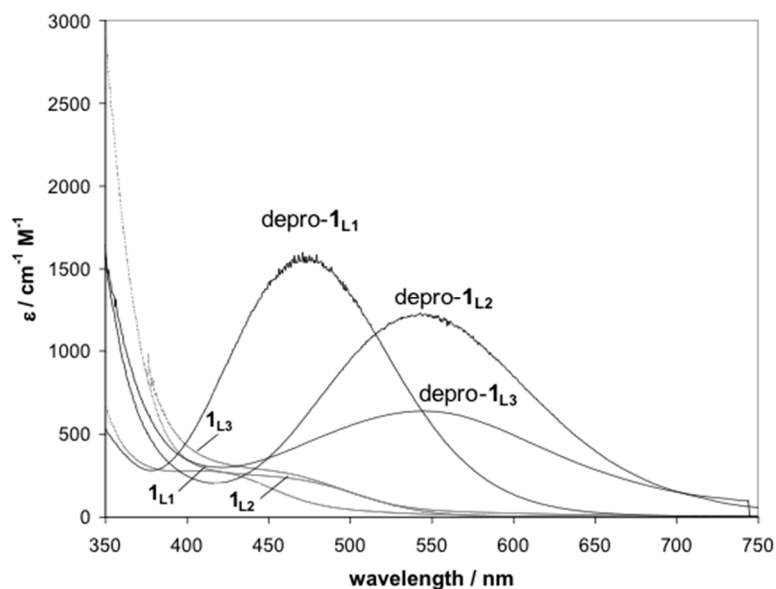


Figure 4. Electronic spectra of deprotonated aryl-Cu^{III} intermediates (depro-1_{L1}, depro-1_{L2}, depro-1_{L3}) UV-Vis plots for aryl-Cu^{III} complexes [(L_x)Cu^{III}]²⁺, *x* = 1–3 (1_{L1}–1_{L3}) are also shown in the plot.

The lower yield obtained is related to the fact that the reaction of [(L₂-H)Cu^I](OTf) (2_{L2-H}) with O₂ first undergoes an oxidation to Cu^{II}, which enables it to then undergo a C-H activation through a disproportionation reaction (50% aryl-Cu^{III} and 50% Cu^I). Therefore, route b converges with route a (Figure 2) and the obtaining of the low 25% yield for 3_{L2} through route b, compared to the 65% obtained through route a (Figure 2), mainly stems from the disproportionation pathway.

3. Materials and Methods

All reagents and solvents were purchased from Sigma Aldrich (Saint Louis, MO, USA) and used without further purification. Cu^{III} complexes [(L_x)Cu^{III}](X)₂ (*x* = 1–3; X = ClO₄⁻, OTf⁻, PF₆⁻) [16,23], and Cu^I complexes [(L₁-H)Cu^I](OTf) (2_{L1-H}), [(L₂-H)Cu^I](OTf) (2_{L2-H}) and [(L₃-H)Cu^I](OTf) (2_{L3-H}) were synthesized following reported procedures [41]. NMR data concerning product identity were collected with a Bruker 400 AVANCE (Billerica, MA, USA). Preparation and handling of air-sensitive Cu^I complexes were carried out in a N₂ drybox. High resolution mass spectra (HRMS) were recorded on a Bruker MicrOTOF-Q IITM instrument (Billerica, MA, US) using ESI-MS at Serveis Tècnics University of Girona.

Warning: Although we have experienced no problems with the compounds reported herein, perchlorate salts are potentially explosive, and should only be handled in small quantities and never heated in a solid state.

[(L₁-O)₂Cu^{II}](OTf)₂ (3_{L1}-(OTf)₂): the synthesis was carried out under N₂. Into a solution of complex 1_{L1}-(OTf)₂ (0.05 g, 8.7 × 10⁻⁵ mol) in CH₃CN (1 mL) was injected a KOH(aq) 1M (87 μL, 8.7 × 10⁻⁵ mol). Reaction was stirred until the red-brown intermediate formed faded to green (48 h). Diffusion of diethyl ether and overnight storing at -25 °C allowed formation of green crystals in 30% isolated yield (0.012 g). ESI-MS (CH₃CN): 3_{L1} 743 [-(OTf)]⁺, 297 [(L₁-O)Cu^{II}]⁺; UV/Vis (CH₃CN): λ_{max} (ε) = 394 (760), 699 (615); IR (KBr pellet, cm⁻¹): 3258 (m), 3121 (m), 2924 (w), 1591 (w), 1456 (m), 1285 (s),

1252 (s), 1165 (m), 1031 (m), 640 (m); elemental analysis calcd for $C_{26}H_{40}N_6O_2Cu_2(C_2F_6S_2O_6) \cdot 0.5CH_3CN$ (%): C 38.1, H 4.60, N 10.00, S 7.00; found: C 37.95, H 4.82, N 10.22, S 6.75.

Complex $3_{L1}-(OTf)_2$ can also be obtained by O_2 bubbling of the Cu^I complex $[(L_1-H)Cu^I](OTf)$ (2_{L1-H}) (see synthesis of complex 3_{L2}).

$[(L_2-O)_2Cu^{II}](OTf)_2$ ($3_{L2}-(OTf)_2$): Synthesis was carried out under N_2 . Into a solution of complex $1_{L2}-(OTf)_2$ (0.03 g, 4.9×10^{-5} mol) in CH_3CN (2 mL) was injected a $KOH(aq)$ 1M (50 μ L, 5.0×10^{-5} mol). Reaction was stirred until the violet intermediate formed faded to green (2–3 h). Slow diffusion of diethyl ether allowed the formation of green crystals in 65% isolated yield (0.011 g). ESI-MS (CH_3CN): 799 $[3_{L2}-(OTf)]^+$, 325 $[(L_2-O)Cu^{II}]^+$; UV/Vis (CH_3CN): λ_{max} (ϵ) = 411 nm (1000), 765 nm (610); IR (KBr pellet, cm^{-1}): 3258 (m), 3210 (m), 2931 (m), 2869 (m), 1592 (m), 1463 (s), 1282 (s), 1236 (s), 1162 (s), 1022 (s), 636 (s); elemental analysis calcd for $C_{30}H_{48}N_6O_2Cu_2(C_2F_6S_2O_6)$ (%): C 40.50, H 5.10, N 8.80, S 6.70; found: C 40.10, H 5.40, N 8.40, S 6.40.

Perchlorate complex $3_{L2}-(ClO_4)_2$ is synthesized in a similar manner, and X-ray quality crystals of $3_{L2}-(ClO_4)_2 \cdot CH_3CN$ were obtained by recrystallization in $CH_3CN/ether$.

Complex $3_{L2}-(OTf)_2$ can also be obtained by O_2 bubbling of the Cu^I complex $[(L_2-H)Cu^I](OTf)$ (2_{L2-H}). Colorless complex $[(L_2-H)Cu^I](OTf)$ (0.025 g, 5.4×10^{-5} mol) in 2 mL CH_3CN/CH_2Cl_2 1/3 under N_2 is treated with 1.75 mL of dioxygen O_2 (8.4×10^{-5} mol). Solution changes to violet slowly and after 3 h stirring fades to green. Slow diffusion of diethyl ether allowed isolation of bis-phenoxo complex $3_{L2}-(OTf)_2$ in 25% isolated yield.

$[(L_3-O)_2Cu^{II}](OTf)_2$ ($3_{L3}-(OTf)_2$): synthesis was carried out under N_2 . Into a solution of complex $1_{L3}-(OTf)_2$ (0.03 g, 5.05×10^{-5} mol) in CH_3CN (2 mL) was injected a $KOH(aq)$ 1M (50 μ L, 5.0×10^{-5} mol). Reaction was stirred until the violet intermediate formed faded to green (1–2 h). Slow diffusion of diethyl ether allowed the formation of green crystals in 60% isolated yield (0.014 g). ESI-MS (CH_3CN): 771 $[3_{L3}-(OTf)]^+$, 311 $[(L_3-O)Cu^{II}]^+$; UV/Vis (CH_3CN): λ_{max} (ϵ) = 436 nm (830), 756 nm (485); IR (KBr pellet, cm^{-1}): 3336 (m), 3294 (m), 1591 (m), 1465 (m), 1280 (s), 636 (s).

Complex 3_{L3} can also be obtained from oxygenation of the corresponding Cu^I complex: colorless solution of complex $[(L_3-H)Cu^I](PF_6)$ (2_{L1-H}) (0.025 g, 5.57×10^{-5} mol) in 2 mL CH_3CN/CH_2Cl_2 1/3 under Ar is treated with excess O_2 at room temperature. Solution changes to violet and slowly and after 3 h stirring fades to green. Slow diffusion of diethyl ether allowed isolation of bis-phenoxo complex $3_{L3}-(PF_6)_2$ in 20% isolated yield. ESI-MS (CH_3CN): 767 $[3_{L3}-(PF_6)]^+$, 311 $[(L_3-O)Cu^{II}]^+$. Elemental analysis calcd for $C_{28}H_{44}N_6O_2Cu_2P_2F_6$ (%): C 36.80, H 4.90, N 9.20; found: C 37.09, H 5.11, N 9.10.

X-ray diffraction analysis. The measurement was carried out on a BRUKER SMART APEX CCD diffractometer (Billerica, MA, US) using graphite-monochromated Mo $K\alpha$ radiation ($\lambda = 0.71073$ Å). CCDC 2027155 ($3_{L1}-(OTf)_2$), 2027156 ($3_{L2}-(ClO_4)_2 \cdot CH_3CN$), 2027157 ($3_{L3}-(PF_6)_2$) contain the supplementary crystallographic data for this paper.

4. Conclusions

In summary, seven well-defined aryl- Cu^{III} complexes featuring different ring sizes and different electronic properties have been reacted with water in basic conditions to produce intriguing bis-phenoxo- Cu^{II}_2 complexes (3_{L1} – 3_{L6}), all of which are characterized by XRD. A structural trend correlating the size of the macrocycle and the geometry of each metal center is found, where the smaller 12-membered macrocycle ring (L_4) favors square-pyramidal geometry, whereas 13-membered (L_1) and 14-membered macrocyclic rings (L_2 – L_3) favored trigonal bipyramidal geometries [39]. Mechanistic investigations indicate that the reaction takes place by an initial deprotonation of the NH group coordinated to Cu^{III} center, subsequent reductive elimination with H_2O as nucleophile to form phenoxo products, and finally air oxidation of the Cu^I produced to form the final bis-phenoxo- Cu^{II}_2 complexes, whose enhanced stability acts as a thermodynamic sink and pushes the reaction forward. Furthermore, the corresponding $[(L_x-H)Cu^I](OTf)$ (2_{Lx-H}) complexes react with O_2 to undergo $1e^-$ oxidation to Cu^{II} and subsequent C-H activation via disproportionation to form aryl- Cu^{III} species, which then undergo the same reaction path towards bis-phenoxo- Cu^{II}_2 complexes. Facile formation of bis-phenoxo- Cu^{II}_2

complexes through aryl-Cu^{III} reductive elimination with basic water is shown, and also the formal aromatic hydroxylation of arene substrates (L_x-H) via aryl-Cu^{III} is mechanistically unraveled.

Supplementary Materials: The following are available online, Figures S1 and S2. Figure S1: ¹H NMR changes in [(L₁-H)Cu^I](OTf) (2_{L1-H}) complex spectrum after O₂ bubbling, Figure S2: ESI-MS of complex depro-1_{L1}.

Author Contributions: Conceptualization, X.R.; methodology and formal analysis, R.X., X.F. and X.R.; writing—original draft preparation and editing, X.R.; funding acquisition, X.R. All authors have read and agreed to the published version of the manuscript.

Funding: This research was funded by MINECO-Spain, CTQ2016-77989-P.

Acknowledgments: X.R. is grateful for an ICREA-Acadèmia award. We thank STR UdG for technical support.

Conflicts of Interest: The authors declare no conflict of interest.

References

1. Ley, S.V.; Thomas, A.W. Modern synthetic methods for copper-mediated C(aryl)-O, C(aryl)-N, and C(aryl)-S bond formation. *Angew. Chem. Int. Ed.* **2003**, *42*, 5400–5449. [[CrossRef](#)] [[PubMed](#)]
2. Tye, J.W.; Weng, Z.; Giri, G.; Hartwig, J.F. Copper(I) phenoxide complexes in the etherification of aryl halides. *Angew. Chem. Int. Ed.* **2010**, *49*, 2185–2189. [[CrossRef](#)] [[PubMed](#)]
3. Tye, J.W.; Weng, Z.; Johns, A.M.; Incarvito, C.D.; Hartwig, J.F. Copper complexes of anionic nitrogen ligands in the amidation and imidation of aryl halides. *J. Am. Chem. Soc.* **2008**, *130*, 9971–9983. [[CrossRef](#)] [[PubMed](#)]
4. Shafir, A.; Lichtor, P.A.; Buchwald, S.L. N-versus O-arylation of aminoalcohols: Orthogonal selectivity in copper-based catalysts. *J. Am. Chem. Soc.* **2007**, *129*, 3490–3491. [[CrossRef](#)]
5. Maiti, D.; Buchwald, S.L. Orthogonal Cu- and Pd-based catalyst systems for the O- and N-arylation of aminophenols. *J. Am. Chem. Soc.* **2009**, *131*, 17423–17429. [[CrossRef](#)]
6. Jones, G.O.; Liu, P.; Houk, K.N.; Buchwald, S.L. Computational explorations of mechanisms and ligand-directed selectivities of copper-catalyzed ullmann-type reactions. *J. Am. Chem. Soc.* **2010**, *132*, 6205–6213. [[CrossRef](#)]
7. Casitas, A.; Ribas, X. The role of organometallic copper(III) complexes in homogeneous catalysis. *Chem. Sci.* **2013**, *4*, 2301–2318. [[CrossRef](#)]
8. Evano, G.; Blanchard, N.; Toumi, M. Copper-mediated coupling reactions and their applications in natural products and designed biomolecules synthesis. *Chem. Rev.* **2008**, *108*, 3054–3131. [[CrossRef](#)]
9. Jiang, Y.; Ma, D. Modern Ullmann-Goldberg chemistry: Arylation of N-nucleophiles with aryl halides. In *Copper-Mediated Cross-Coupling Reactions*; Evano, G., Blanchard, N., Eds.; Wiley: Hoboken, Germany, 2014.
10. Ribas, X.; Güell, I. Cu(I)/Cu(III) catalytic cycle involved in Ullmann-type cross-coupling reactions. *Pure Appl. Chem.* **2014**, *86*, 263–467. [[CrossRef](#)]
11. Casitas, A.; King, A.E.; Parella, T.; Costas, M.; Stahl, S.S.; Ribas, X. Direct Observation of Cu^I/Cu^{III} Redox Steps Relevant to Ullmann-Type Coupling Reactions. *Chem. Sci.* **2010**, *1*, 326–330. [[CrossRef](#)]
12. Yao, B.; Wang, D.-X.; Huang, Z.-T.; Wang, M.-X. Room-temperature aerobic formation of a stable aryl-Cu(III) complex and its reactions with nucleophiles: Highly efficient and diverse arene C-H functionalizations of azacalix[1]arene[3]pyridine. *Chem. Commun.* **2009**, 2899–2901. [[CrossRef](#)] [[PubMed](#)]
13. Yao, B.; Wang, Z.-L.; Zhang, H.; Wang, D.-X.; Zhao, L.; Wang, M.-X. Cu(ClO₄)₂-mediated arene C-H bond halogenations of azacalixaromatics using alkali metal halides as halogen sources. *J. Org. Chem.* **2012**, *77*, 3336–3340. [[CrossRef](#)] [[PubMed](#)]
14. Wang, Z.-L.; Zhao, L.; Wang, M.-X. Construction of Caryl–Calkynyl Bond from Copper-Mediated Arene–Alkyne and Aryl Iodide–Alkyne Cross-Coupling Reactions: A Common Aryl-Cu(III) Intermediate in Arene C–H Activation and Castro–Stephens Reaction. *Org. Lett.* **2012**, *14*, 1472–1475. [[CrossRef](#)] [[PubMed](#)]
15. Wang, Z.-L.; Zhao, L.; Wang, M.-X. Caryl–Calkyl bond formation from Cu(ClO₄)₂-mediated oxidative cross coupling reaction between arenes and alkyllithium reagents through structurally well-defined Ar-Cu(III) intermediates. *Chem. Commun.* **2012**, *48*, 9418–9420. [[CrossRef](#)] [[PubMed](#)]
16. Ribas, X.; Jackson, D.A.; Donnadiou, B.; Mahía, J.; Parella, T.; Xifra, R.; Hedman, B.; Hodgson, K.O.; Llobet, A.; Stack, T.D.P. Aryl C-H Activation by Cu(II) To Form an Organometallic Aryl-Cu(III) Species: A Novel Twist on Copper Disproportionation. *Angew. Chem. Int. Ed.* **2002**, *41*, 2991–2994. [[CrossRef](#)]

17. Rovira, M.; Font, M.; Acuna-Pares, F.; Parella, T.; Luis, J.M.; Lloret-Fillol, J.; Ribas, X. Aryl-copper(III)-acetylides as key intermediates in Csp²-Csp model couplings under mild conditions. *Chem. Eur. J.* **2014**, *20*, 10005–10010. [[CrossRef](#)] [[PubMed](#)]
18. Rovira, M.; Font, M.; Ribas, X. Model Csp²-Csp³ Hurtley Coupling Catalysis that Operates through a Well-Defined CuI/CuIII Mechanism. *ChemCatChem* **2013**, *5*, 687–691. [[CrossRef](#)]
19. Casitas, A.; Canta, M.; Solà, M.; Costas, M.; Ribas, X. Nucleophilic Aryl Fluorination and Aryl Halide Exchange Mediated by a Cu(I)/Cu(III) Catalytic Cycle. *J. Am. Chem. Soc.* **2011**, *133*, 19386–19392. [[CrossRef](#)]
20. King, A.E.; Huffman, L.M.; Casitas, A.; Costas, M.; Ribas, X.; Stahl, S.S. Copper-Catalyzed Aerobic Oxidative Functionalization of an Arene C-H Bond: Evidence for an Aryl-Copper(III) Intermediate. *J. Am. Chem. Soc.* **2010**, *132*, 12068–12073. [[CrossRef](#)]
21. Casitas, A.; Poater, A.; Solà, M.; Stahl, S.S.; Costas, M.; Ribas, X. Molecular mechanism of acid-triggered aryl-halide reductive elimination in well-defined aryl-Cu^{III}-halide species. *Dalton Trans.* **2010**, *39*, 10458–10463. [[CrossRef](#)]
22. Bernoud, E.; Company, A.; Ribas, X. Direct use of CO₂ for O-arylcarbamate synthesis via mild Cu(II)-catalyzed aerobic C-H functionalization in pincer-like macrocyclic systems. *J. Organomet. Chem.* **2017**, *845*, 44–48. [[CrossRef](#)]
23. Xifra, R.; Ribas, X.; Llobet, A.; Poater, A.; Duran, M.; Solà, M.; Stack, T.D.P.; Benet-Buchholz, J.; Donnadiu, B.; Mahía, J.; et al. Fine-Tuning the Electronic Properties of Highly Stable Organometallic CuIII Complexes Containing Monoanionic Macrocyclic Ligands. *Chem. Eur. J.* **2005**, *11*, 5146–5156. [[CrossRef](#)] [[PubMed](#)]
24. Rovira, M.; Jasikova, L.; Andris, E.; Acuna-Pares, F.; Soler, M.; Guell, I.; Wang, M.-Z.; Gomez, L.; Luis, J.M.; Roithova, J.; et al. A CuI/CuIII prototypical organometallic mechanism for the deactivation of an active pincer-like CuI catalyst in Ullmann-type couplings. *Chem. Commun.* **2017**, *53*, 8786–8789. [[CrossRef](#)]
25. Rovira, M.; Soler, M.; Güell, I.; Wang, M.-Z.; Gómez, L.; Ribas, X. Orthogonal Discrimination among Functional Groups in Ullmann-Type C–O and C–N Couplings. *J. Org. Chem.* **2016**, *81*, 7315–7325. [[CrossRef](#)] [[PubMed](#)]
26. Huffman, L.M.; Casitas, A.; Font, M.; Canta, M.; Costas, M.; Ribas, X.; Stahl, S.S. Observation and Mechanistic Study of Facile C–O Bond Formation between a Well-Defined Aryl-Copper(III) Complex and Oxygen Nucleophiles. *Chem. Eur. J.* **2011**, *17*, 10643–10650. [[CrossRef](#)]
27. Monnier, F.; Taillefer, M. Catalytic C–C, C–N and C–O Ullmann-Type Coupling Reactions. *Angew. Chem. Int. Ed.* **2009**, *48*, 6954–6971. [[CrossRef](#)] [[PubMed](#)]
28. ten Brink, G.J.; Arends, I.W.C.E.; Sheldon, R.A. The Baeyer–Villiger Reaction: New Developments toward Greener Procedures. *Chem. Rev.* **2004**, *104*, 4105–4124. [[CrossRef](#)]
29. Galli, C. Radical reactions of arenediazonium ions: An easy entry into the chemistry of the aryl radical. *Chem. Rev.* **1988**, *88*, 765–792. [[CrossRef](#)]
30. Anderson, K.W.; Ikawa, T.; Tundel, R.E.; Buchwald, S.L. The Selective Reaction of Aryl Halides with KOH: Synthesis of Phenols, Aromatic Ethers, and Benzofurans. *J. Am. Chem. Soc.* **2006**, *128*, 10694–10695. [[CrossRef](#)]
31. Yu, C.-W.; Chen, G.S.; Huang, C.-W.; Chern, J.-W. Efficient Microwave-Assisted Pd-Catalyzed Hydroxylation of Aryl Chlorides in the Presence of Carbonate. *Org. Lett.* **2012**, *14*, 3688–3691. [[CrossRef](#)]
32. Maurer, S.; Liu, W.; Zhang, X.; Jiang, Y.; Ma, D. An Efficient Synthesis of Phenol via CuI/8-Hydroxyquinoline-Catalyzed Hydroxylation of Aryl Halides and Potassium Hydroxide. *Synlett* **2010**, *2010*, 976–978. [[CrossRef](#)]
33. Xu, H.-J.; Liang, Y.-F.; Cai, Z.-Y.; Qi, H.-X.; Yang, C.-Y.; Feng, Y.-S. CuI-Nanoparticles-Catalyzed Selective Synthesis of Phenols, Anilines, and Thiophenols from Aryl Halides in Aqueous Solution. *J. Org. Chem.* **2011**, *76*, 2296–2300. [[CrossRef](#)] [[PubMed](#)]
34. Fier, P.S.; Maloney, K.M. Reagent Design and Ligand Evolution for the Development of a Mild Copper-Catalyzed Hydroxylation Reaction. *Org. Lett.* **2017**, *19*, 3033–3036. [[CrossRef](#)] [[PubMed](#)]
35. Shin, E.-J.; Kwon, G.-T.; Kim, S.-H. Room-Temperature Ionic Liquids (RTILs) as Green Media for Metal- and Base-Free ipso-Hydroxylation of Arylboronic Acids. *Synlett* **2019**, *30*, 1815–1819. [[CrossRef](#)]
36. Zhang, Y.-H.; Yu, J.-Q. Pd(II)-Catalyzed Hydroxylation of Arenes with 1 atm of O₂ or Air. *J. Am. Chem. Soc.* **2009**, *131*, 14654–14655. [[CrossRef](#)]

37. Ribas, X.; Calle, C.; Poater, A.; Casitas, A.; Gómez, L.; Xifra, R.; Parella, T.; Benet-Buchholz, J.; Schweiger, A.; Mitrikas, G.; et al. Facile C-H Bond Cleavage via a Proton-Coupled Electron Transfer Involving a C-H...Cu^{II} Interaction. *J. Am. Chem. Soc.* **2010**, *132*, 12299–12306. [[CrossRef](#)]
38. Addison, A.W.; Rao, T.N.; Reedijk, J.; Van Rijn, J.; Verschoor, G.C. Synthesis, structure, and spectroscopic properties of copper(II) compounds containing nitrogen-sulfur donor ligands: The crystal and molecular structure of aqua[1,7-bis(*N*-methylbenzimidazol-2'-yl)-2,6-dithiaheptane]copper(II) perchlorate. *J. Chem. Soc. Dalton Trans.* **1984**, *7*, 1349–1356. [[CrossRef](#)]
39. Fusi, V.; Llobet, A.; Mahía, J.; Micheloni, M.; Paoli, P.; Ribas, X.; Rossi, P. A new Cu(I) complex that mimics the cresolase reaction of tyrosinase. Crystal structure of its oxygenated Cu(II) complex. *Eur. J. Inorg. Chem.* **2002**, *2002*, 987–990. [[CrossRef](#)]
40. Casitas, A.; Ioannidis, N.; Mitrikas, G.; Costas, M.; Ribas, X. Aryl-O reductive elimination from reaction of well-defined aryl-Cu(III) species with phenolates: The importance of ligand reactivity. *Dalton Trans.* **2011**, *40*, 8796–8799. [[CrossRef](#)]
41. Ribas, X.; Xifra, R.; Parella, T.; Poater, A.; Solà, M.; Llobet, A. Regiospecific C-H Bond Activation: Reversible H/D Exchange Promoted by CuI Complexes with Triazamacrocyclic Ligands. *Angew. Chem. Int. Ed.* **2006**, *45*, 2941–2944. [[CrossRef](#)]

Sample Availability: Samples of the compounds **3_{L1}**–**3_{L3}** are available from the authors.



© 2020 by the authors. Licensee MDPI, Basel, Switzerland. This article is an open access article distributed under the terms and conditions of the Creative Commons Attribution (CC BY) license (<http://creativecommons.org/licenses/by/4.0/>).